Paper No. 1930. (quote when citing this article)
Eleventh World Conference on Earthquake Engineering
ISBN: 0 08 042822 3

FURTHER INVESTIGATION ON SEISMIC RESPONSE OF SOIL AND EMBEDDED STRUCTURE IN HUALIEN LSST PROGRAM

TERUYUKI UESHIMA* and HAJIME OKANO**

*Earthquake Engineering Department, Abiko Research Laboratory,
Central Research Institute of Electric Power Industry(CRIEPI)
1646 Abiko, Abiko-City, Chiba Prefecture, 〒270-11, JAPAN
** Architectural Research and Development Department,
Technical Research and Development Institute, Kumagai Gumi Co.,Ltd.
1043 Ooaza-Onigakubo, Tukuba-City, Ibaraki Prefecture, 〒300-22, JAPAN

ABSTRACT

International joint program, Large-Scale Seismic Test Program at Hualien, Taiwan (called 'HLSST' for short, hereafter) is ongoing, to observe the dynamic behaviors of soil-structure system subjected to big earthquakes (Tang *et al.* 1991). Examining the seismic records, the noticeable discrepancy between the NS and EW components of transfer functions of soil stratum is observed consistently in every downhole array and in every seismic record obtained up to now. In this paper, the method is presented to estimate the azimuth of the principal axes of the soil stratum based on the theoretical consideration, and soil properties of principal axes are estimated by system identification method. It is also studied whether the peak frequency shift toward lower frequency range recognized in the transfer function of the structure top over the ground surface is caused by the soil nonlinearity or not.

KEYWORD

Anisotropy; Coherence; Input-Output Relation; System Identification; Seismic Observation; Downhole Array; PS logging; Soil-Structure Interaction; Hualien LSST Program.

INTRODUCTION

In 'HLSST' Program, a large-scale containment model with about 1/4th of commercial nuclear power plant was constructed on the gravelly layers in seismically active Hualien, Taiwan, the detailed site soil investigations and the forced vibration tests of the containment model were carried out, and seismic observation of the soil-structure system started in June, 1993.

Examining the seismic records, some unsettled phenomena are found to be included. Firstly, the NS-component of transfer function of the downhole array is obviously different from the EW-component. This discrepancy is observed consistently in all of the three downhole arrays, and moreover, observed consistently in all of the seismic records obtained up to now. Secondly, the transfer function of the structure top over the ground surface has plural predominant frequencies, which do not always agree with the fundamental frequency of the soil-structure system detected from the forced vibration test (Morishita *et al.*,1993-1994).

In this paper, the theoretical input-output relation for the anisotropic soil stratum is derived in order to comprehend its dynamic behavior and the method is presented to estimate the azimuth of the principal axes. Then, the soil properties for the principal axes are estimated by the system identification.

The origin of the plural peaks recognized in the transfer function of the structure top over the ground surface is also studied . Lastly, it is examined whether the peak frequency shift toward the lower frequency range in the transfer function of the structure top is caused by the soil nonlinearity or not.

OUTLINE OF THE SEISMIC OBSERVATION

'HLSST' deploys the surface array and the three downhole arrays. Fig.1 shows the configuration of the downhole array, together with the properties of 'the unified ground model' (called 'UMFVT2' for short hereafter) obtained from the detailed site soil geotechnical investigation (Kokusho *et al.*, 1994). Three downholes are named DHAj (j=1,3) respectively as shown in Fig.1. Table.1 lists the seismic records observed up to now. In the following studies, EQ2 & EQ4 are mainly used as the typical ones. In the examination of the effect of the soil nonlinearity, EQ6 is referred as the largest one recorded up to now.

Table 1 Observed Earthquakes

Eq. No.	Date	Magnitude (M)	Epi-center (km)	Focal Depth (km)	Max. Acc. (gal) RFEL	A15L
EQ1	16/09/'93	4.2	7.6	21.1	32.9	11.6
EQ2	20/01/'94	5.6	24.4	49.5	71.3	32.2
EQ3	30/05/'94	4.5	9.6	18.5	37.6	34.1
EQ4	05/06/'94	6.2	54.0	5.3	64.7	41.8
EQ5	23/02/'95	5.8	21.8	21.7	53.8	48.9
EQ6	01/05/'95	4.9	4.6	8.4	166.6	134.8
EQ7	02/05/'95	4.6	1.7	8.9	72.8	87.9

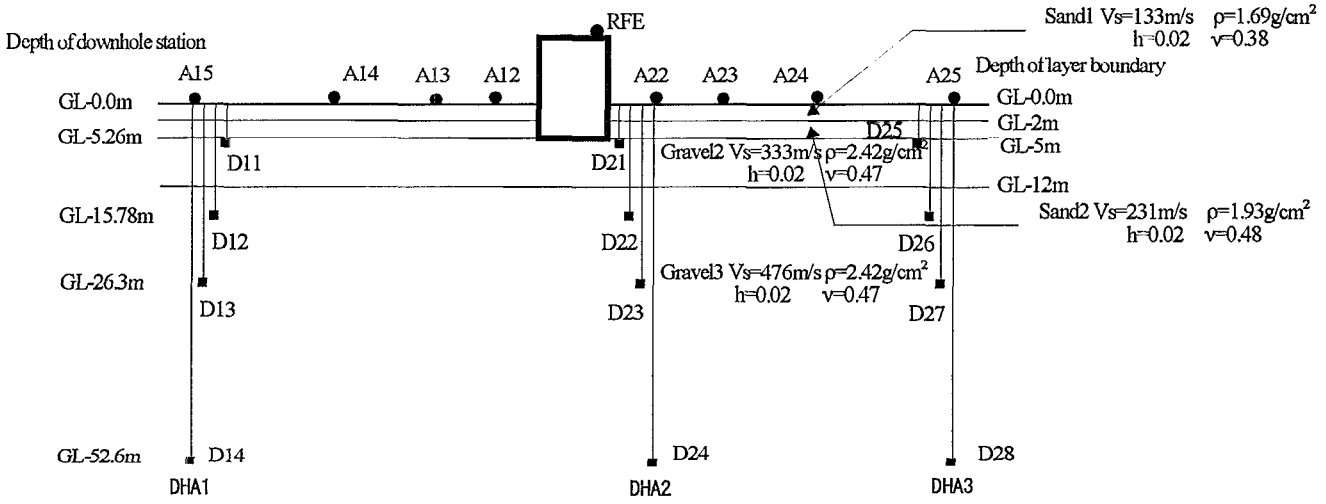

Fig.1 Configuration of Downhole Array and Unfied Ground Model 'UMFVT2'

ANISOTROPY OF THE TRANSFER FUNCTION IN DOWNHOLE ARRAY

Fig.2 shows the transfer function of the ground surface over the deepest downhole station for all the downhole arrays, during EQ2 & EQ4. The solid line shows L(NS)-component, and the dashed line shows T(EW)-component. In case the records of ground surface were unavailable, the records of downhole stations near the surface were substituted. Transfer functions are computed from the cross spectra, where each of the denominator and the numerator is passed through Parzen's window with the bandwidth of 0.2 Hz. Fig.2 indicates that each predominant frequency for T-component is obviously lower than the corresponding one for L-component in every downhole array.

The orbit of each station in DHA1 is compared in order to check the influence of azimuth instrumentation error (Fig.3). Each record is passed through the low-pass filter with cut-off frequency of 0.3Hz to remove the dynamic amplification factor. Although the slight deviations are observed in A15 and D12, the azimuth instrumentation error seems negligible, indicating that it is no more the cause of the observed anisotropy.

It is considered that the discrepancy of transfer function between the L-component and the T-component is reflecting the certain ground condition extending some wide area, because the phenomenon is observed consistently in every downhole array and in all of the seismic records listed in Table.1. In the following sections, theoretical input-output relation of anisotropic soil stratum is derived to comprehend its dynamic behavior.

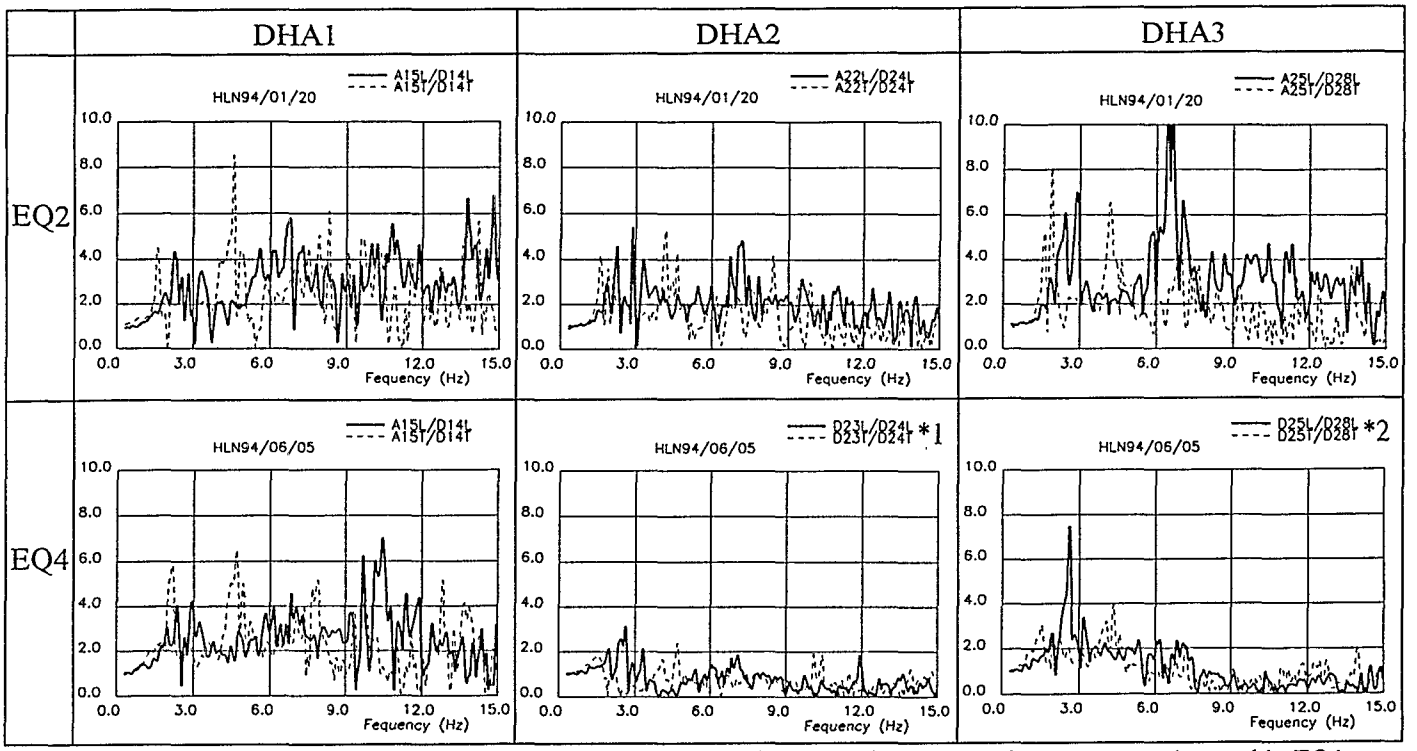

(*1,*2) D23 and D25 was used respectively, because corresponding ground surface stations were not observed in EQ4.

Fig.2 Transfer Function of Downhole Array (Ground Surface/Deepest Station)

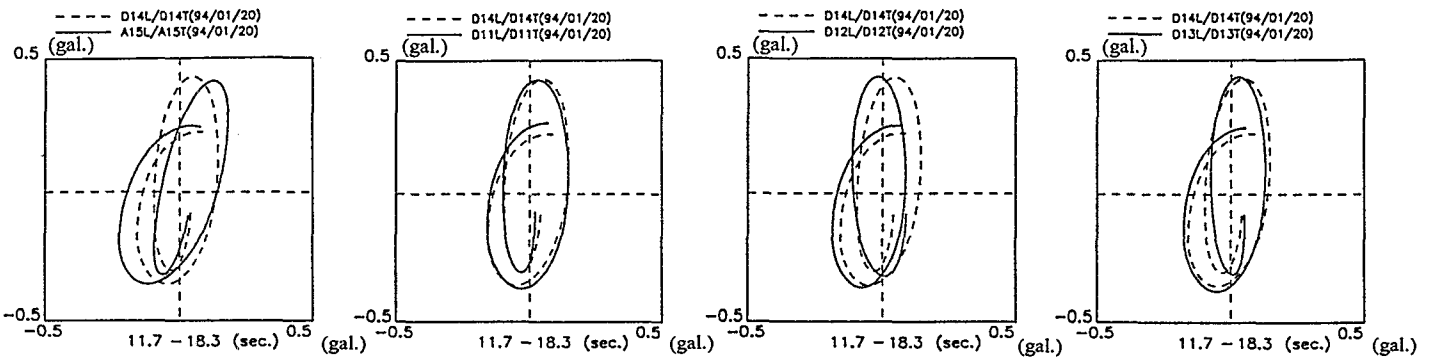

Fig3 Orbit of Low Frequency Component (fc=0.3Hz) in Downhole DHA1during EQ2

Statistical Input-Output Relation of Anisotoropic Soil Stratum

Here, the soil strata are assumed to have the principal axes consisting of strong and weak axes orthogonal to each other, and the coordinate system (x,y) coincides with principal axes. Input-output relations in the principal axes are given as follows;

$$S_{IxOx}(\omega) = \frac{1}{2\pi}\int_{-\infty}^{\infty} R_{IxOx}(\tau)e^{-i\omega\tau}d\tau = \frac{1}{2\pi}\int_{-\infty}^{\infty}\int_{-\infty}^{\infty} h_x(\eta)E[f_{Ix}(t)f_{Ix}(t+\tau-\eta)]e^{-i\omega\tau}d\eta d\tau \qquad (1a)$$

$$= H_x(\omega)S_{IxIx}(\omega)$$

$$S_{IyOy}(\omega) = \frac{1}{2\pi}\int_{-\infty}^{\infty} R_{IyOy}(\tau)e^{-i\omega\tau}d\tau = \frac{1}{2\pi}\int_{-\infty}^{\infty}\int_{-\infty}^{\infty} h_y(\eta)E[f_{Iy}(t)f_{Iy}(t+\tau-\eta)]e^{-i\omega\tau}d\eta d\tau \qquad (1b)$$

$$= H_y(\omega)S_{IyIy}(\omega)$$

where,

$R_{I\varsigma o\varsigma}(\tau)$: cross-correlation function between input and output in ζ-axis $E[\,]$: expectation

$f_\varsigma(t)$: time-history in ζ-axis $h_\varsigma(t)$: impulse response function in ζ-axis

$H_\varsigma(\omega)$: transfer function in ζ-axis $S_{I\varsigma O\varsigma}(\omega)$: cross-spectrum between input and output in ζ-axis

$S_{I\varsigma I\varsigma}(\omega)$: power-spectrum of input in ζ-axis $S_{O\varsigma O\varsigma}(\omega)$: power-spectrum of output in ζ-axis

Then, the seismic motion is considered to be observed in the coordinates (x', y'), which make the angle of θ from the principal axes. Time-histories in terms of the principal axes are transformed to those in terms of the observation coordinate system as follows;

$$\begin{Bmatrix} f_{x'}(t) \\ f_{y'}(t) \end{Bmatrix} = \begin{bmatrix} \cos\theta & \sin\theta \\ -\sin\theta & \cos\theta \end{bmatrix} \begin{Bmatrix} f_x(t) \\ f_y(t) \end{Bmatrix} \tag{2}$$

Substituting equation (2) into (1), after some algebraic efforts, cross-spectrum between input and output in the observation coordinate system is derived as follows;

$$S_{Ix'Ox'}(\omega) = \left[\frac{1}{2}H_x(\omega)\{(1+\cos 2\theta) - \sin 2\theta \frac{S_{Ix'Iy'}(\omega)}{S_{Ix'Ix'}(\omega)}\} + \frac{1}{2}H_y(\omega)\{(1+\cos 2\theta) + \sin 2\theta \frac{S_{Ix'Iy'}(\omega)}{S_{Ix'Ix'}(\omega)}\}\right] S_{Ix'Ix'}(\omega) \tag{3}$$

Equation (3) signifies that the cross-spectrum of input-output is influenced not only by both directional transfer functions but also by the input motion orthogonal to the output direction in terms of cross-spectrum of the orthogonal components of input motion, unless the observation coordinates agree with the principal axes. That is, the dynamic response in x'-direction is affected by the input motion in y'-direction.

Using the power-spectrum of the output in the observation coordinates which is derived in a similar manner, the coherence function between the input and the output in the observation coordinates is given as follows;

$$\begin{aligned} coh^2_{Ix'Ox'}(\omega) &= \frac{\left|S_{Ix'Ox'}(\omega)\right|^2}{S_{Ix'Ix'}(\omega)S_{Ox'Ox'}(\omega)} \\ &= \frac{[\frac{1}{4}\{H_x(\omega)-H_y(\omega)\}^*\{H_x(\omega)-H_y(\omega)\}(1-\cos 4\theta)coh^2_{Ix'Iy'}(\omega)S_{Iy'Iy'}(\omega)+A(\omega)]}{[\frac{1}{4}\{H_x(\omega)-H_y(\omega)\}^*\{H_x(\omega)-H_y(\omega)\}(1-\cos 4\theta)S_{Iy'Iy'}(\omega)+A(\omega)]} \end{aligned} \tag{4}$$

where,

$$\begin{aligned} A(\omega) &= H_x^*(\omega)H_x(\omega)[\cos^4\theta S_{Ix'Ix'}(\omega) - \cos\theta^3\sin\theta\{S_{Ix'Iy'}(\omega)+S_{Iy'Ix'}(\omega)\}] \\ &+ H_y^*(\omega)H_y(\omega)[\sin^4\theta S^2_{Ix'Ix'}(\omega) + \cos\theta\sin^3\theta\{S_{Ix'Iy'}(\omega)+S_{Iy'Ix'}(\omega)\}] \\ &+ H_x^*(\omega)H_y(\omega)[\cos^2\theta\sin^2\theta\{S_{Ix'Ix'}(\omega) + \cos\theta^3\sin\theta S_{Ix'Iy'}(\omega) - \cos\theta\sin^3\theta S_{Iy'Ix'}(\omega)] \\ &+ H_y^*(\omega)H_x(\omega)[\cos^2\theta\sin^2\theta\{S_{Ix'Ix'}(\omega) - \cos\theta\sin^3\theta S_{Ix'Iy'}(\omega) + \cos^3\theta\sin\theta S_{Iy'Ix'}(\omega)] \end{aligned} \tag{4'}$$

and * denotes complex conjugate. Taking the following self-evident relation into account,

$$\{H_x(\omega)-H_y(\omega)\}^*\{H_x(\omega)-H_y(\omega)\} \geq 0 \tag{5}$$

$$coh^2_{Ix'Iy'}(\omega) \leq 1$$

the coherence $coh^2_{Ix'Ox'}(\omega)$ given by the equation (4) becomes the periodical function with the period of π /2, taking maximum value when θ=0, π/2, so far as the coherence $coh^2_{Ix'Iy'}(\omega)$ between two orthogonal

input motions is constant in regard to the rotation of the coordinate system. It suggests that the direction of the principal axes could be estimated from this periodical variation of $coh^2_{Ix'Ox'}(\omega)$, so long as the fluctuation of $coh^2_{Ix'Iy'}(\omega)$ is small.

Fig.4 shows examples of the variation of $coh^2_{Ix'Ox'}(\omega)$. The coherence was computed using Parzen's window with the bandwidth of 0.2 Hz, and the average from 0.3Hz to 10.0Hz was plotted. Each coherence shows periodical variation with the period of about $\pi/2$ as expected from the equation (4), each of which takes the maximum value when the coordinate rotation angle take the value around -5°～-15°. As the variation of each $coh^2_{Ix'Iy'}(\omega)$ does not agree with the variation of $coh^2_{Ix'Ox'}(\omega)$, the variation of the latter function is proved not to be caused by that of the former function. The shape of the transfer function along the principal axes (Fig.5) seems more definite than the one along the axes which makes 45° from the principal axes (Fig.6), which gives the supporting evidence for the validity of the above mentioned estimation of principal axes.

The strong axis of the soil stratum is estimated to be -10°(-5°～-15°), that is, about 10° east from the magnetic north. The direction of the strong axis is approximately parallel to the coastal line of Taiwan.

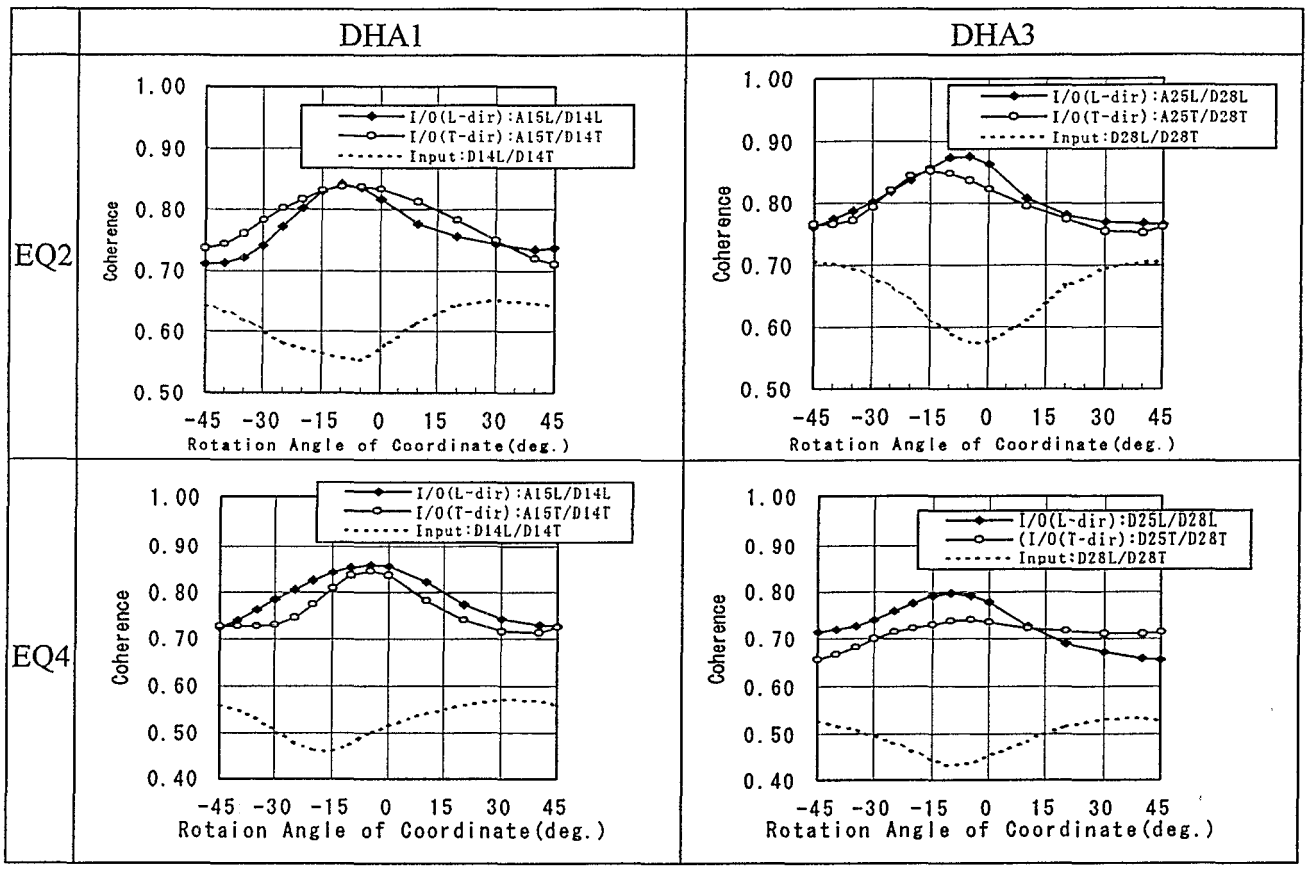

Fig.4 Coherence versus Rotation Angle of Coordinates (Average from 0.3Hz to 10.0Hz)

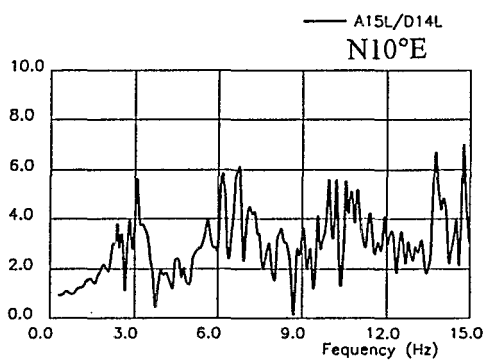

Fig.5 Transfer Function along Principal Axes

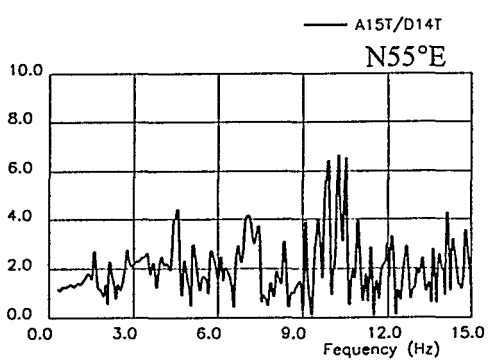

Fig.6 Transfer Function along coordinates Rotated 45° from Principal Axes

Identification of Soil Properties

The system identification was carried out to estimate the soil properties along the principal axes. Powell's hybrid method (Nakagawa *et al.*, 1982) was employed, where the steepest descent method and Gauss-Newton method are hybrid. Jacobian matrix of the transfer functions for the soil column was calculated by the perturbation method. In the course of the inversion analysis, the shear wave velocities (Vs_j) and the damping constants (h_j) are dealt as the target parameters at the same time, and the iteration of the convergence was repeated until the reduction rate of the square sum of the errors and the variation rates for all the target parameters become less than 1% simultaneously.

Identified soil properties of the strong and the weak axes are shown in Table.2 and 3 respectively.

Table 2 Identified Soil Properties of Strong Axis(N10°E)

Layer	UMFVT2(PS Lggng.) Vs (m/s)	ρ (t/m3)	h (%)	EQ2:20/01/'94 Vs (m/s)	h (%)	EQ4:05/06/'94 Vs (m/s)	h (%)	Average Vs (m/s)	h (%)	Ratio of Vs
Layer1*1: GL0.0～-5.0m	192	1.83	2	208	9.7	210	12.4	209	11.1	1.09
Layer2*2: GL-5.0～-12.0m	333	2.42	2	332	6.3	349	11.5	341	8.9	1.02
Layer3*3: GL-12.0m～-52.6m	476	2.42	2	487	12.8	451	10.4	469	11.6	0.99

Table 3 Identified Soil Properties of Weak Axis(N80°W)

Layer	UMFVT2(PS Lggng.) Vs (m/s)	ρ (t/m3)	h (%)	EQ2:20/01/'94 Vs (m/s)	h (%)	EQ4:05/06/'94 Vs (m/s)	h (%)	Average Vs (m/s)	h (%)	Ratio of Vs
Layer1*1: GL0.0～-5.0m	192	1.83	2	182	12.3	184	13.7	183	13.0	0.95
Layer2*2: GL-5.0～-12.0m	333	2.42	2	197	11.5	205	14.0	201	12.8	0.60
Layer3*3: GL-12.0m～-52.6m	476	2.42	2	355	10.4	360	13.3	358	11.9	0.75

*1:Sand1 & Sand2 in Fig.1 *2:Gravel2 in Fig.1 *3:Gravel3 in Fig.1

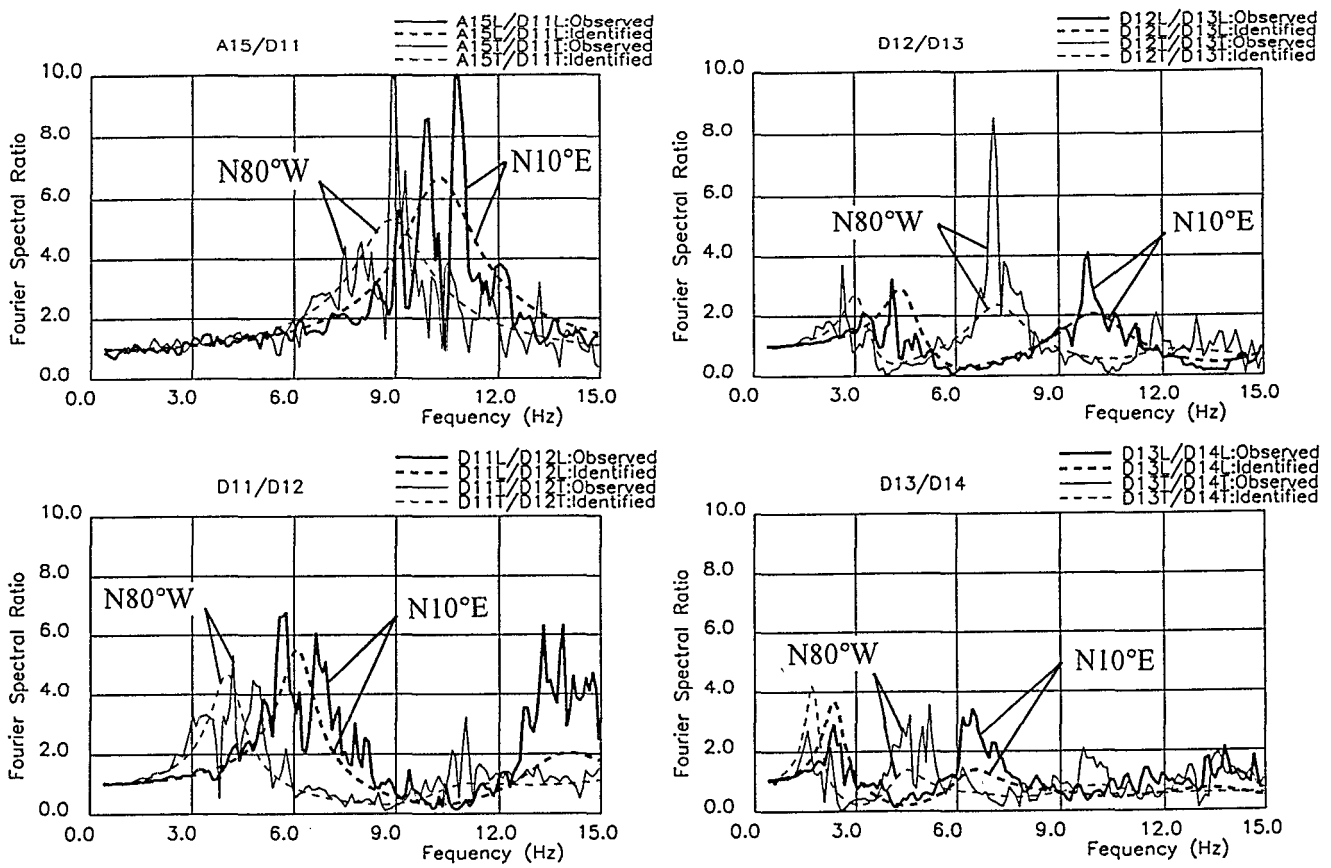

Fig.7 Observed Transfer Function and Final Result of System Identification (EQ2)

The soil properties in 'UMFVT2' obtained by downhole/crosshole method was used as a set of the initial values in both cases. Fig.7 shows the identified transfer functions. The sand properties of two layers shallower than GL.-5m are put into one set of the properties in order to make the convergence computation stable. The identified values of Vs along the strong axis almost agrees with those of 'UMFVT2'. On the contrary, the identified Vs for gravelly layers (Layer2&3 in Tables.2&3) along the weak axis are 25～40% slower than those of 'UMFVT2', although there is no much difference between the identified and the initial Vs for the sand layer (Layer1). Therefore, it can be said that the ground anisotropy emerged in the transfer function is striking in the gravelly layers. With regard to the above-mentioned, it may be suggestive to take note of Tanaka Y. *et al.* (1995) where it is reported that the shear wave velocity of the gravel obtained by means of cyclic triaxial test is considerably slower than the one obtained by means of shear wave logging in laboratory test. These phenomena were not expected at first, because any remarkable ununiformity or inhorizontality around this site had not been reported in the geotechnical/geological surveys.

It is worth while to note that the identified set of Vs for the strong axis almost agrees with the set of Vs in 'UMFVT2'. This fact suggests that Vs obtained by the general geotechnical method, such as PS logging, where the arrival time of the wave is measured, is apt to result in that of the strong axis unless the measurement direction agrees with the weak axis.

CHARACTERISTICS OF STRUCTURAL BEHAVIOR SUBJECTED TO EARTHQUAKES

Fig.8 shows an example of the transfer function of the structure top over the ground surface, along the coordinates rotated by the factor of 30° east from the magnetic north, so that the rotated axis agrees approximately with the principal axes detected from FVT after backfill (Morishita *et al.*, 1994). The solid line in Fig.8 is the transfer function computed from the cross-spectrum, and the dashed line in Fig.8 is the one computed from the power-spectrum. Fig.8 exhibits complexity of the structure response having plural peaks. The peak at 4.7 Hz in L-component which is striking in the transfer function computed from the power-spectrum is not so remarkable in the one from the cross-spectrum. This fact implies that the random fluctuation of the phase occurs around this frequency range. Taking into account that the second predominant frequency of the T-component of the soil stratum is around 4.7 Hz(Fig.2&6), this peak is considered to be influenced by the input motion orthogonal to the output direction following what is meant by the equation (3). These phenomena are considered to be the supporting evidence of the existence of the ground anisotropy.

Table4 Resonant Frequency of Soil-Structure System

	N30°E (Hz)	N60°W (Hz)
FVT2	6.3	6.1
EQ2	5.6	5.5
EQ4	6.0	5.6
EQ6	5.0	5.4

Table5 Result of Equivalent Linear Analysis

Layer	Max. Strain(%)			Reduction Rate of Vs(%)		
	EQ2	EQ4	EQ6	EQ2	EQ4	EQ6
GL0.0～-2.0m	0.0019	0.0025	0.0101	2.1	3.2	11.0
GL-2.0～-5.0m	0.0018	0.0022	0.0088	2.3	2.9	10.1
GL-5.0～-12.0m	0.0016	0.0015	0.0890	4.0	3.7	17.4

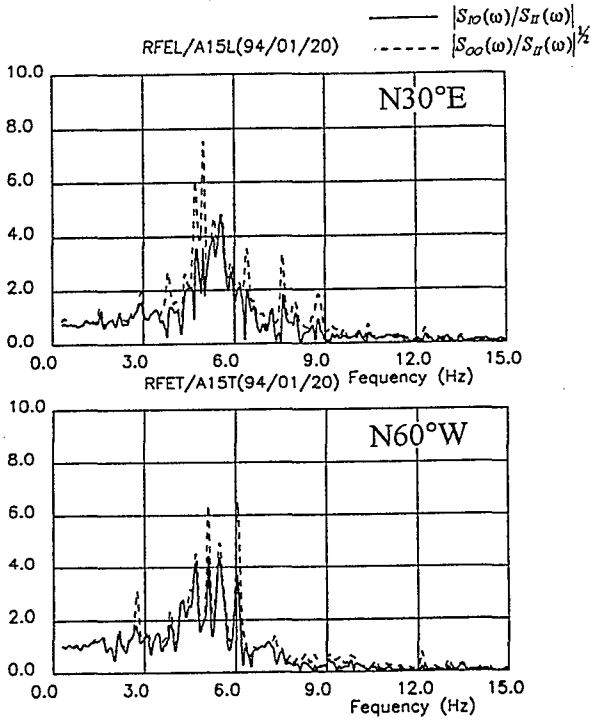

Fig.8 Transfer Function of Structure top over A15(EQ2)

Excluding such apparent peaks, Table4 lists predominant frequencies emerging in the transfer function computed from cross-spectrum for EQ2, 4 & 6 after the coordinate rotation. The predominant frequencies during the seismic events are slightly lower than the fundamental frequency detected by the forced vibration test. The one-dimensional equivalent linear analysis by the program 'SHAKE' was performed. The initial soil properties are the ones in 'UMFVT2'(Fig.1). The Vs reduction rates in Table5 appear insufficient to thoroughly interpret the predominant frequency shift in Table4, but soil nonlinearity seems to constitute a part of the causes of the frequency shift emerging in the transfer function of the structure top over the ground surface.

CONCLUSIONS

Concluding remarks of this study are as follows:

1) The anisotropy in transfer functions is observed consistently in all of the three downhole arrays and in all the seismic records obtained up to now.
2) From the theoretical consideration, it is shown that the coherence between input and output takes the maximum value when the observation coordinates coincide with the principal axes, and take the minimum value when the observation coordinates make the angle of 45° from the principal axes.
3) The variation of coherence indicates that the angle of the strong axis of soil stratum is 10° east from the magnetic north at the Hualien site. The Vs of the free field soil layers for the strong axis estimated by the system identification almost agree with those of the ground model 'UMFVT2' obtained by the downhole method. On the contrary, the identified Vs for gravelly layers along the weak axis are 25～40% slower than those of 'UMFVT2'.
4) Apparent peaks sometimes emerge in the transfer function of the structure top over the ground surface of which the frequencies are obviously different from the fundamental system frequency detected by means of FVT, especially when transfer functions are calculated from power spectrum. It is also made clear that some of such apparent peaks are caused by the ground anisotropy.
5) According to the result of the one-dimensional equivalent linear analysis, the predominant frequency shift of the soil-structure system observed during relatively large earthquakes may be explained by the soil nonlinearity to a certain extent.

ACKNOWLEDGMENTS

The authors would like to acknowledge the researchers in the Electric Power Research Institute, USA, Taiwan Power Company, etc. for their cooperation in the 'HLSST' program.

REFERENCES

Kokusho, T. *et al.* (1994). Soil-structure interaction research of a large-scale model structure at Hualien, Taiwan :(Part 1) Evaluation of S-wave velocity of foundation ground around a model building for numerical analysis. *9th Japan Earthquake Engineering Symposium (JEES).*

Morishita, H. *et al.* (1993-1994). Forced vibration test of Hualien large scale soil-structure interaction model (Part 1-5). *Annual Meeting of Architectural Inst. of Japan.*

Nakagawa, T. , Koyanagi, Y. (1982). *Analysis of Experimental Data by Least Sum of Square Method.* (Tokyo University Press.)

Tanaka, T. *et al.*(1995), Evaluation of initial shear modulus of gravelly soil by laboratory test and PS-logging. *First International Conference on Earthquake Geotechnical Engineering(IS-TOKYO '95)*, pp.101-106.

Tang, H. T. *et al.* (1991). The Hualien large- scale seismic test for soil-structure interaction research. *11th SMiRT. K04/4* pp.69-74.

Ueshima, T. *et al.* (1995). Large-Scale Seismic Test for Soil-Structure Interaction Research in Hualien, Taiwan. *ICONE.*